Heliyon 9 (2023) e19961

Contents lists available at ScienceDirect

Heliyon

journal homepage: www.cell.com/heliyon

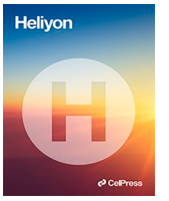

Numerical study of different ventilation schemes in a classroom for efficient aerosol control

Ainara Ugarte-Anero [a,b,c], Unai Fernandez-Gamiz [a,b,c,*], Koldo Portal-Porras [a], Jose Manuel Lopez-Guede [b,c,d], Gaspar Sanchez-Merino [b,c]

[a] Nuclear Engineering and Fluid Mechanics Department, University of the Basque Country, UPV/EHU, Nieves Cano 12, Vitoria-Gasteiz, 01006, Araba, Spain
[b] Bioaraba, New Technologies and Information Systems in Health Research Group, Vitoria-Gasteiz, Spain
[c] Osakidetza Basque Health Service, Araba University Hospital, Medical Physics Department, Vitoria-Gasteiz, Spain
[d] System Engineering and Automation Control Department, University of the Basque Country, UPV/EHU, Nieves Cano 12, Vitoria-Gasteiz, 01006, Araba, Spain

ARTICLE INFO

Keywords:
Computational fluid mechanics (CFD)
Natural ventilation
Mechanical ventilation
Droplets
Fate
Evaporation
Sneezing
Flow
COVID-19

ABSTRACT

The air quality is a parameter to be controlled in order to live in a comfortable place. This paper analyzes the trajectory of aerosols exhaled into the environment in a classroom. Three scenarios are investigated; without ventilation, with natural and with mechanical ventilation. A multiphase computational fluid study based on Eulerian-Lagrangian techniques is defined. Temperature and ambient relative humidity, as well as air velocity, direction and pressure is taken into account. For droplets evaporation, mass transfer and turbulent dispersion have been added. This work tends to be of great help in various areas, such as the field of medicine and energy engineering, aiming to show the path of aerosols dispersed in the air. The results show that the classroom with a mechanical ventilation scheme offers good results when it comes to an efficient control of aerosols. In all three cases, aerosols exhaled into the environment impregnate the front row student in the first 0.5 s. Reaching the time of 4, 2 and 1 s, in the class without ventilation, mechanical and natural ventilation, respectively, the aerosols have been already deposited on the table of the person in the first row, being exposed for longer in the case of no ventilation. Particles with a diameter of less than 20 μm are distributed throughout the classroom over a long period. The air jet injected into the interior space offers a practically constant relative humidity and a drop in temperature, slowing down the process of evaporation of the particles. In the first second, it can be seen that a mass of 0.0025 mg formed by 9 million droplets accumulates, in cases without ventilation and natural ventilation. The room with a mechanical installation accumulated 5.5 million particles of mass 0.0028 mg in the first second. The energy losses generated by natural ventilation are high compared to the other scenarios, exactly forty and twenty times more in the scenario with mechanical ventilation and without ventilation, respectively.

* Corresponding author. Nuclear Engineering and Fluid Mechanics Department, University of the Basque Country, UPV/EHU, Nieves Cano 12, Vitoria-Gasteiz, 01006, Araba, Spain.
E-mail address: unai.fernandez@ehu.eus (U. Fernandez-Gamiz).

https://doi.org/10.1016/j.heliyon.2023.e19961
Received 28 October 2022; Received in revised form 11 July 2023; Accepted 7 September 2023
Available online 7 September 2023

1. Introduction

Health is very important state to take care of, and more nowadays, after the situation of risk experienced worldwide in the last three years because of the COVID-19 pandemic. The isolation of people infected with minor symptoms was the protocol to follow for that infected person not to spread the virus, a norm marked by the World Health Organization (WHO). Due to the isolation, in an enclosed space, the air quality could get worse due to the contaminated load generated by the isolated person [1]. Most of the time, humans reside in closed spaces, such as offices, universities or at home, among others. That is why improving air quality means better welfare for humans [2]. On the contrary, an airless environment generates unpleasant and harmful situation for health, since it increases the contagion of aerial diseases, as indicated by Ref. [3]. Studies such as Ref. [4] show that indoor spread and infection of the virus is more likely to spread than outdoors due to exposure time. According to Ref. [5] indoor environmental quality depends, among other factors, on thermal comfort. This term is divided into two large groups; relative humidity and ambient temperature. For instance, studies as Ref. [6] shows that a project on the dynamics of a single droplet of saliva, indicates that both, ambient temperature and relative humidity, are parameters that directly affect the evaporation time of the drops of a human sneeze. Therefore, more time in the environment implies lower air quality and a greater chance of infection. On the other hand, the study of Agarwal et al. [5] reports that, there are improvement techniques to take care of the safety of an isolated patient infected by COVID-19. Focusing on engineering controls highlights ventilation, both natural and mechanical. In particular, simple ventilation is the one that offers a higher probability of infection according to Ref. [7].

Natural ventilation consists of the renovation of the internal air by using doors, windows or ducts. Homes that do not have mechanical ventilation use these techniques to improve indoor air quality. Table 1 shows a summary of works similar to the one presented in this paper, with its objective and concluded results. The computational study of Ref. [8] displays that each building is unique and requires a specific study in order to calculate a good ventilation inside the house. The mathematical study of Ref. [9] simulates nine scenarios of natural ventilation of a classroom and ensures that, the height where the air inlet window is installed and the difference in height inlet-air outlet is a factor that significantly affects the renewal of the indoor air. The CFD outcomes of the inquiry of Ref. [10] demonstrates that the combination of the interior air of the passenger compartment and the movement of the person promotes an internal flow field difficult to solve. Computational simulations of Zhou et al. [11] present that, natural ventilation is a reliable technique for air renewal as it achieves reasonably good results, even so, including a mechanical ventilation installation would be essential to achieve better effects. As a result, airborne sneezing could spread to adjacent classrooms with an average infection rate of about 11%. In contrast, mechanical ventilation introduces the renewal of the air inside a cabin thanks to the function of a fan. The numerical work performed by Ref. [12] consists of a study room with 30 students and a teacher with different air inlet speeds. They show that after sneezing, as the air velocity increases, the concentration of particles exhaled into the environment decreases. It is also remarkable, that with a low air inlet speed the person in the first row is the most at risk of infection. Instead, with higher regeneration air inlet speed the people in the last rows are the most exposed, with a particle concentration of 2.48×10^{-9} kg/m^3. Increasing the renewed air intake to 100% for about an hour causes a reduction in aerosol mass of 80%, which means that the probability of infection is reduced to 50%, according to the model of CFD performed by Ref. [13]. The numerical study of Ref. [14], whose domain is composed of a classroom of 24 student and a teacher, ensures that if the teacher is infected the probability of contagion in the classroom is 100% for certain student. Proven the effectiveness of this ventilation technique, Ref. [15] ensures that the best strategy to reduce to almost negligible levels of risk of infection would be the combination of external air 100% and UV-C (ultraviolet-C) in ventilation ducts.

Table 1
Various research studies on the subject presented in this paper. Objectives and results of similar studies.

Title	Objetive and Results	Reference
Numerical modeling of a sneeze, a cough and a continuum speech inside a hospital lift	The numerical evaluation of the efficiency of the ventilator installed in a hospital elevator was the objective set by the authors of this work. Their results showed that, after a cough, the fan was able to absorb 60% of smaller aerosols	[14]
CFD Analyses: The Effect of Pressure Suction and Airflow Velocity on Coronavirus Dispersal	Through CFD, the authors of this research wanted to make an evaluation of the ventilation system of a university hospital. Rooms with air velocity, dispersion and gas mixing increased the probability of leakage and made it possible to spread to other uncontaminated places	[15]
Computational Fluid Dynamic (CFD), air flow-droplet dispersion, and CO_2 analysis for healthy public spaces configuration to comply with COVID 19 protocol	The main objective of this work was to see the behavior of airflow inside a room that is composed of closed and independent seats. It was concluded that by increasing both space and distance the risk of contagion decreased	[16]
COVID-19 spread in a classroom equipped with partition – A CFD approach	A numerical study that analyzes a classroom at three different air inlet speeds with a ventilation system to observe the effect of aerosol droplet dispersion. Decreasing the air velocity of the ventilation decreases the velocity obtained by these droplets, thus increasing the exposure time	[11]
Airborne transmission of COVID-19 and mitigation using a box fan air cleaners in a poorly ventilated classroom	The goal of this work is to create a simulation of a classroom equipped with a horizontal unit fan to observe its performance. The results show that the installation of fans is of great help reducing the risk of transmission area	[17]
Ventilation CFD analysis at a classroom as a tool for air safety verification under COVID19 context, a case study	The aim of this study was to see that implementing small changes or installing a forced flow mechanism, helps largely to renew the air within a classroom with 300 students. The mechanical ventilation system gives better results eliminating contaminated air	[18]

Finally, the work in Ref. [16], notes that installing a portable air cleaner of descending flow placed in the middle of the classroom is the most efficient configuration to reduce the spread of infectious diseases airway.

As has been observed, ventilation is an important factor for controlling airborne diseases. However, the over-steer generates energy losses that seriously affect both, the habitability of space and the energy efficiency of this. The concept of energy is recurrent not only by professionals in the energy sector, but by a large majority of society. The media open every day with news about the price of electricity or about the supply of natural gas in Europe. First, the global ralentization in industrial activity as a result of COVID-19, the payment of CO_2 emission allowances and the invasion of Ukraine have caused a large fluctuation in prices. Variations in demand and limited supply from producer countries have led Europe, dependent on imported natural gas, and Spain in particular, to suffer the rise in energy prices. The average price of electricity in the wholesale market has varied from 47.68 €/MWh in 2019 to 111.85 €/MWh in 2021 in Spain, showing a sharp rise, [17]. Considering the effects of rising energy costs on industry or domestic users, the European Commission and the Spanish central government have taken a number of measures to mitigate the rise in prices, such as the REPowerEU plan, which aims to ensure the minimum filling of 90% of natural gas storage or the Iberian derogation setting a price cap on gas used to produce electricity. In addition to these measures, energy consumption must be reduced, ensuring thermal comfort. Energy efficiency aims at this end, optimizing the energy resource to achieve certain levels of satisfaction with the thermal environment and ensuring the comfort of its occupants. The optimal design of a room has been taken into account since ancient times, the solar gain through the orientation to the south, the materials and the type of structure are chosen according to the climatic zone, as well as the required isolation. Ventilation is another factor that has a leading role in the design of buildings. A detailed analysis of the situation and needs of the environment, prevents heat losses and as a consequence decreases the consumption of both thermal and electrical equipment [18].

This work aims to study, through computational fluid mechanics techniques, the different ventilation schemes for efficient aerosol control. The stage to be presented is a classroom composed of a teacher and nine students. The teacher, through speech, generates aerosols, and a student placed in the second-row sneezes. First, the dispersion and deposition of exhaled aerosols is observed, without ventilation. Next, the same scenario is shown, but this time with two doors and three windows open at the back of the class, simulating a natural ventilation. The path of these particles is examined. The last computational simulation to present is replacing natural ventilation by mechanical ventilation. The final result is the energy losses that are generated in the process, the heat transfer of the different ventilation strategies and the path that these aerosols travel in the 3 proposed scenarios. It checks which scenario is the most efficient to avoid contagion.

2. Materials and methods

2.1. Computational domain and initial conditions

Implementing computational fluid mechanics techniques to solve complex problems, for example, the path and fate of particles released into the environment by humans, the following situation has been considered. This study entails of a university classroom of 8.5 × 7 × 3.1 m (X, Y, Z). Inside the classroom, there are nine students in three rows of three students, separated by 1.5 m between them, regulatory distance for the non-contagion of diseases by air, as confirmed by Ref. [19] in their mathematical study. In the beginning of the classroom, the teacher is placed, separated from the first row of students 1.5 m away. The height of the teacher and the students are 1.76 and 1.45 m, respectively. Fig. 1 shows the described geometry. The computational domain is an indoor temperature of 21 °C and a relative humidity of 42% at an atmospheric pressure. Table 2 displays the computational domain measures.

The classroom has been modeled where the teacher gives the lesson. For that purpose, the teacher's mouth has been modeled as a cone-shaped injector with an inclination of 15°, and expels to the environment aerosols produced by the flow of speech. In this case, the student infected shall be placed in the second row on the right. The sneeze produced by the student has been simulated by a cone-shaped injector of 45°, geometry approximate to the shape the mouth takes when a human sneezes, according to Ref. [20]. The sneezing speed takes a sinusoidal curve of 450 ms, according to experimental results of Ref. [21]. Fig. 2 shows the sinusoidal curve of the sneezing speed, reaching a maximum value of 70 m/s. The results of Ref. [22] show that the diameter of the particles by the sneeze, follow a lognormal distribution with a standard deviation of 1.5. Fig. 3 displays the distribution that follows, with a range of 0–1000 μm, where the mean value is placed at a diameter of 360.1 μm.

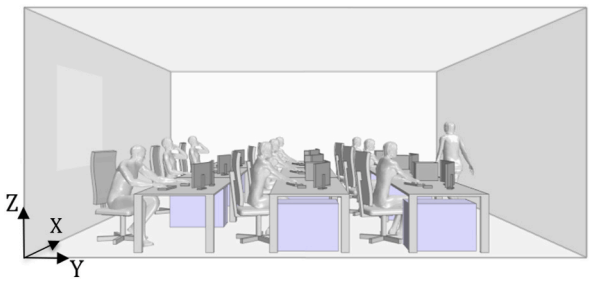

Fig. 1. Computational domain geometry. Measurements; X = 8.5 m, Y = 7 m and Z = 3.1 m. The classroom is maintained at a temperature of 21 °C and a relative humidity of 42% at constant atmospheric pressure.

Table 2
Computational domain measures.

Parameter	Value
Width	8.5 m
Length	7 m
Height	3.1 m
Teacher's height	1.76 m
Student's height	1.45 m
Distance between students	1.5 m
Distance between rows	1.5 m
Distance between first row and teacher	1.5 m
Number of students	9
Number of rows	3
Number of students in each row	3
Number of windows	3
Number of doors	2
Window height	2.3 m
Window width	2 m
Door height	2 m
Door width	1 m
Number of slits	8
Number of lids	2
Slit area	0.05 m^2
Lid area	1.6 m^2

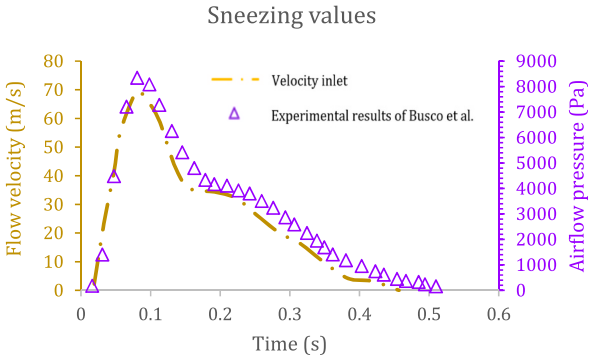

Fig. 2. Sinusoidal graph following sneezing flow. Experimental project data of Ref. [21] with a maximum value of 70 m/s.

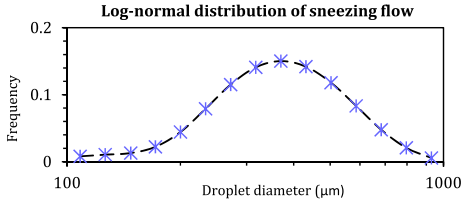

Fig. 3. Lognormal distribution of sneezing flow. The particle diameter range takes values from 0 to 1000 μm with an average value of 360.1 μm with a standard deviation of 1.5.

Conversely, the speech has been modeled with a constant velocity of 4 m/s throughout the simulation, according to the study of Ref. [23]. This previous mentioned work understand that speech follows an irregular form, but can be assimilated to a continuous flow. Like sneezing flow, experimental results from Ref. [24] show that speech is assimilated to a log-normal distribution, with a range of 0–600 μm and a mean particle value of 16 μm. Ref. [25] provides a thorough analysis of how the droplet size fits a lognormal curve. The mass generated in speech and sneezing low is 0.33 mg and 6.7 mg, respectively. Although, the mass generated follows a sinusoidal function, as the experimental study of Ref. [26] confirmed, the mean mass that a human expels in a sneeze takes a value of 6.7 mg of saliva. Fig. 4 shows the human sneeze flow diagram.

The contaminated and the speech aerosols produced by the teacher have been inserted at a temperature of 36 °C, i.e., the average temperature of the human body. The mathematical study of Ref. [27] included these conditions in his work. The temperature of the aerosols begins to decrease as they take the atmosphere inside, as shown in Ref. [28]. Even though, saliva is composed of very different

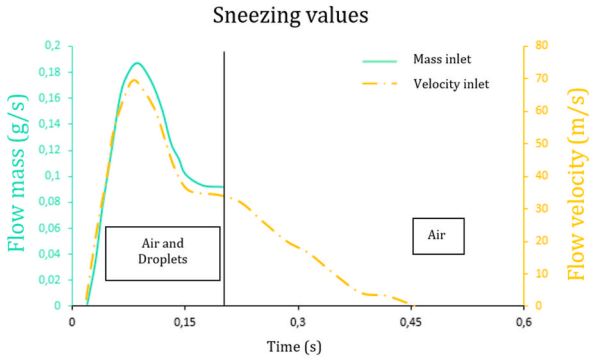

Fig. 4. Sinusoidal graph following sneezing flow. Flow values to simulate the action of a sneeze.

elements, in this study it has been simplified. The expelled fluid is modeled as a physiological saline solution, approximately 0.9% w/v, validated in the study of Ref. [29]. Fig. 5 displays in detail which student is infected and the injectors.

For a second scenario with natural ventilation, it has been included to the domain previously explained windows and doors. At the back of the classroom, with a width of 2 m and a height of 2.3 m, three windows have been modeled in the domain. The gap between them is 0.5 m. In the opposite wall of the classroom, at both ends, two doors have been placed of 2 m high and 1 m wide. Fig. 6 shows this new geometry simulating a classroom with natural ventilation. The air enter through the windows, inlet boundary, at a speed of 2.7 m/s with an external temperature of 17 °C, a relative humidity of 80% and an atmospheric pressure. The wind speed value corresponds to a very weak breeze. Studies like Ref. [27] and Ref. [20] introduce to their studies speeds of up to 15 km/h, called light winds. In addition, it has been found that in the study of Ref. [30] the wind speed has a value of 2 m/s, very close to the one introduced in this paper.

A third scenario has been set up to see the efficiency of mechanical ventilation. Consequently, a mechanical ventilation system has been installed in the same domain. This ventilation system shall consist of two ducts. Each duct has been modeled with four slits of 0.05 m^2 with an air renewal rate of 6 ACH. According to the American standard ASHRAE 62.1 for classrooms, with 6 air renewals, the

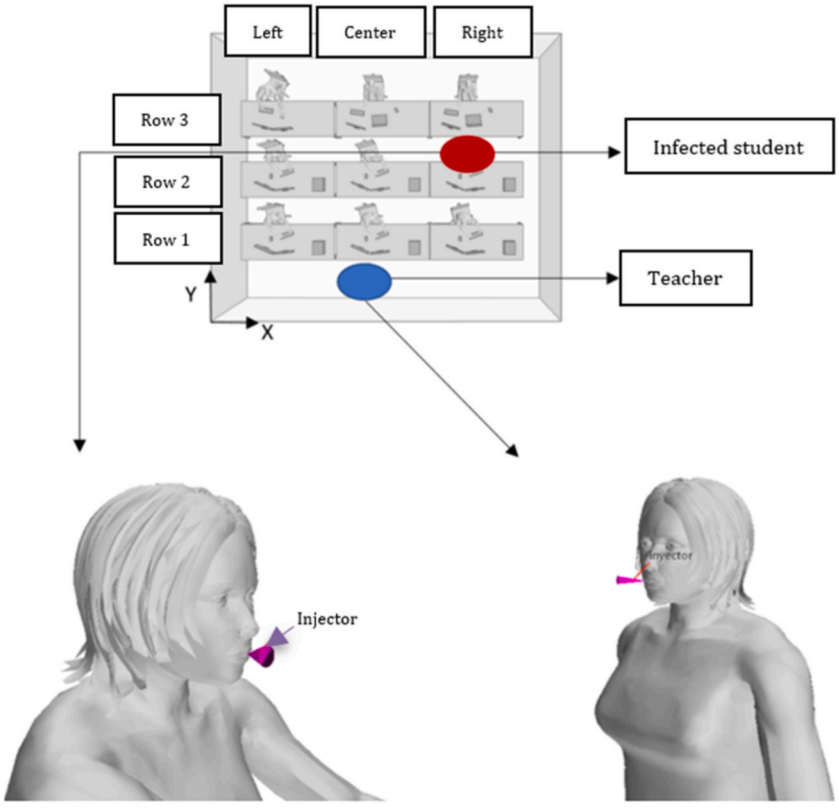

Fig. 5. Injectors to simulate the flow of speech and sneezing. Classroom geometry central view where the infected student and teacher are specified.

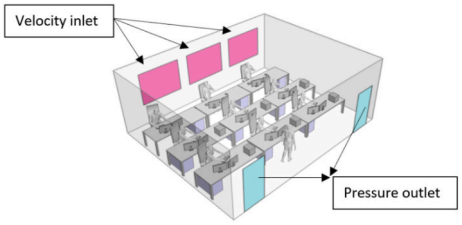

Fig. 6. Geometry of the classroom implementing doors and windows. The windows act as an inlet for clean air and through the doors the polluted air leaves the classroom.

ambient is in an excellent level of ventilation. The slits have been modeled as an inlet boundary, more specific as flow inlet with a value of 0.31 m^3/s. On the dame plate, a 1.6 m^2 lid has been added to absorb the contaminated air found in the room. The absorption pressure exerted by this conduit is the atmospheric pressure, Ref. [31]. Fig. 7 shows a sketch of the geometry that takes this new situation. Table 3 indicates a summary of all the CFD parameters included in the simulation to configure this model.

A trimmer mesh has been used to make the discretization of the domain of this geometry, the same mesh for the three scenarios. Three control volumes have been created, bringing the total to 10.5^6 (10,513,886) cells. As shown in Fig. 8, the created control volumes have to be more detailed; more precision is needed around the mouth.

Governing equations.

The commercial software CFD Star-CCM + has been used to define and solve the numerical problems that have been defined to study the behavior of aerosols. Composed of two phases, in the cases consisting of ventilation, either natural or mechanical, the Eularian phase reaches stability once the air begins to renew. The indoor air that runs through the classroom, as well as the breeze that enters through the windows, is considered a biphasic flow, composed of dry air and water vapor, non-reactive species with the same speed, pressure and temperature properties. Properties such as density and viscosity are the parameters that differentiate these two species, among others. These numerical values have been taken from the Annex of Ref. [32]. To calculate the union of the two circulating species in the so-called air, the mathematical study of Ref. [21] integrates Equation (1) to calculate the union of these, based on the mass weighted mixing method.

$$\varphi_{mix} = \sum_{i=1}^{N=2} \varphi_i Y_i \tag{1}$$

where N refers to the number of components in the mixture. φ_i is the value of the property to be determined for the component of the mixture and Y_i is the mass fraction of dry air and water vapor.

The Navier-Stokes (RANS) equations averaged by Reynolds with the k-ω Shear Stress Transport (SST) turbulence model, developed by Ref. [33], have been introduced into this work. The UpWind algorithm was used for the pressure-speed coupling and a second-order linear wind scheme was used to discretize the mesh. Equations (2) and (3) show the transport formula for kinetic energy and the dissipation ratio.

$$\frac{\partial}{\partial t}(\rho k) + \nabla \bullet (\rho k \bar{v}) = \nabla \bullet [(\mu + \sigma_k \mu_t)\nabla k] + P_k - \rho \beta^* f_{\beta *}(\omega k - \omega_0 k_0) + S_k \tag{2}$$

$$\frac{\partial}{\partial t}(\rho \omega) + \nabla \bullet (\rho \omega \bar{v}) = \nabla \bullet [(\mu + \sigma_\omega \mu_t)\nabla \omega] + P_\omega - \rho \beta^* f_{\beta *}\left(\omega^2 - \omega_0^2\right) + S_\omega \tag{3}$$

where σk, $\sigma \omega$, Pk and P_ω are defined as TP (Terms of Production), instead, Sk and $S\omega$ are the source terms specified by the user. K_0 and

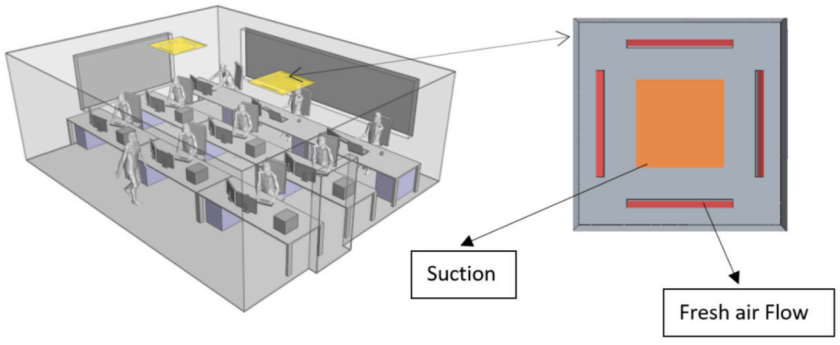

Fig. 7. Classroom geometry implementing mechanical ventilation. Two ducts formed by four spaces that renew the interior air to a flow of 0.31 m^3/s and a duct that is responsible for sucking the polluted air created by humans inhabiting the classroom.

Table 3
Summary of the values included in the model for simulation.

Parameter	Value	Reference
Cone-shape injector	15° and 45°	[20]
Sneeze time	450 ms	[21]
Mass inlet time	220 ms	[21]
Sneeze maximum velocity	70 m/s	[21]
Speech velocity	4 m/s	[23]
Speech mass	0.33 mg	[26]
Sneeze mass	6.7 mg	[26]
Aerosol temperature	36 °C	[27]
Saline solution	0.9% w/v	[29]
Air velocity inlet (natural ventilation)	2.7 m/s	[20,27,30]
Mechanical flow	0.31 m^3/s	[31]

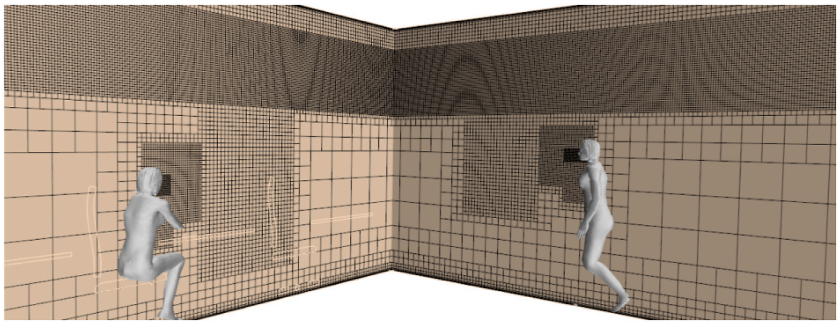

Fig. 8. Cubic meshing created for the discretization of the model to be studied, composed of 10.5^6 cells.

ω_0 are the environmental turbulence values that counteract the decay of the turbulence. On the other hand, $\bar{v}$ is the average speed (m/s), μ is the dynamic viscosity (kg/ms) y $f_{\beta*}$ is the free shear modification factor.

Fluid mechanics is governed by the laws of mass conservation, Equation (4), linear momentum law, Equation (5), and energy law, Equation (6).

$$\frac{\partial \rho}{\partial t} + \nabla \bullet (\rho v) = 0 \tag{4}$$

$$\frac{\partial (\rho v)}{\partial t} + \nabla \bullet (\rho v \otimes v) = \nabla \bullet (pI) + \nabla \bullet T + f_b \tag{5}$$

$$\frac{\partial (\rho E)}{\partial t} + \nabla \bullet (\rho E v) = f_b \bullet v + \nabla \bullet (v \bullet \sigma) - \nabla \bullet q + S_E \tag{6}$$

where ρ is the density (kg/m) and v is the continuous speed (m/s), defining therefore the equation of mass conservation. f_b is the result of the forces of the body per unit of volume acting on the continuous (N/m^3), σ is the tension (N/m^2), p is the pressure (Pa), T is the viscous tensor (kg/ms). Finally, E is the total energy per unit of mass (J/kg), q is the heat flow (J/s) and S_E is one energy source per unit volume (J/m^3).

On the other hand, the Lagrangian phase gives solution to the simulated flow for speech and sneezing. This state is composed of spherical liquid droplets of physiological saline. Subjected to two main forces, such as gravity (m/s) and drag (N), formula that follows Equation (7). The energy follows the Ranz-Marshall correlation.

$$F_d = \frac{1}{2} C_d \rho A_p |v_s| v_s \tag{7}$$

where Cd is the drag coefficient of the drop following the Schiller-Naumann model, A_p is the area of the drop (m^2) and v_s is the sliding speed of the drop (m/s).

Once the droplets are expelled into the air and interact with the medium, the particles, under the effects of surface forces, begin to distort and break. The Taylor Analogy rupture model (TAB) was included in this work in order to take into account the behavior of particles. Another phenomenon that begins to have an effect on particles is the effect of evaporation, due to the temperature difference between droplets and the environment. The quasi-stable model has been implemented in the project to solve this phenomenon. This model consists of drops losing mass, determined by the Sherwood number. Equation (8) expresses the rate of change of the mass of droplets (g/s) due to evaporation.

$$\dot{m}_p = g^* \times A_s \, ln(1+B) \tag{8}$$

where B is the Spalding transfer number, g^* is the mass transfer conductance (g/m^2 s) and A_s is the surface of the drop (m^2). Saturation pressure significantly affects the evaporation effect, according to Ref. [34]. This pressure, being drops composed of a saline solution, is calculated according to Equation (9), also called Raoult's law [29],.

$$P_{va,s} = X_d P_{va}(T_w) \tag{9}$$

where $P_{va,s}$ is the saturation pressure of the drop in the salt mixture (Pa), P_{va} is the equilibrium pressure of the water at a specific temperature (Pa) marked by the Antoine Equation and X_d is the molar fraction of the drop, see Equation (10).

$$X_d = \left(1 + \frac{6 i m_s M_w}{\pi \rho_L M_s \left(d_p\right)^3}\right)^{-1} \tag{10}$$

where M_w and M_s are the molecular weight of water and solute (u), respectively; m_s the mass of solute in the drop (g); d_p the diameter of the drop (m), and the ionic factor, i.

2.2. Validation of the numerical model

A numerical model of CFD needs to be validated with experimental results, obtaining similar result for such validation. As this study is focused on the destination and route that aerosols make due to the currents that can be generated by ventilation, the variable to validate are the path and diameter of the droplet. No experimental studies have been found in the literature that observe the same as indicated in this study. Therefore, experimental studies have been chosen that measure the same variables as our study but instead of a sneeze a single droplet. For this, the phenomenon of evaporation is observed by studying the decrease in the diameter of the droplet as it advances over a closed space. Consequently, the droplet precipitates from a distance of 5 m from the ground and the diameter of the droplet is measured up to a distance of 2.5 m. Therefore, it is assumed that if the CFD results obtained do not show a high error rate among the experimental results, the designed mathematical model is valid. Table 4 shows the error as a percentage between the experimental data and the results obtained with CFD techniques.

The experimental data have been taken from the studies of Ref. [35] and Ref. [36]. The numerical studies of Ref. [6,21,29,37–39] also use this method to validate their work. The study of Ref. [35] consists of two droplets of pure water of 110 μm and 115 μm in diameter with a temperature of 16 °C. These two droplets are introduced into an environment with 70% relative humidity and a temperature of 20 °C and are dropped freely controlling how their diameter decreases as they evaporate progress. Fig. 9 shows the result.

Similarly, the study of Ref. [36] consists of the same, but varying parameters. In this case the diameter of the drop is 170 μm at a temperature of 25 °C in an environment with characteristics of RH = 68% and T_{ext} = 31 °C. Fig. 10 shows the data obtained.

In order to strengthen the validation section, a new analysis has been included. In this case, the evaporation of the pure water particles suspended in the air is studied. For this purpose, the diameter of the particle thrown into the environment (10 μm and 100 μm) is measured to observe the decrease. Evaporation begins when the droplet and the environment meet at different temperatures (370.15 K and 293.15 K, respectively, and RH = 0%). The CFD results obtained were compared with the data provided by Ref. [40] and Ref. [28]. Fig. 11 shows the results obtained, the same process carried out by Refs. [41–44]. The variation obtained between the data used to verify the study and the achieved does not differ excessively.

3. Results

The results obtained are explained in the following subsections.

a. Aerosol route in different scenarios

The influence of ventilation schemes on aerosols route is analyzed. In the following figures, the path of the aerosols exhaled into the environment by the teacher through speech and the student contaminated sneeze, are observed; without ventilation, with natural and

Table 4
Calculated error between the results obtained by CFDs and the experimental data of Ref. [35] and Ref. [36] studies.

Ref. [35] dp = 110 μm	Ref. [35] dp = 115 μm	Ref. [36] dp = 170 μm
0,0003%	0,034%	0,16%
1,15%	0,019%	0,285%
0,39%	0,055%	0,85%
3,6%	0,595%	1,35%
2,7%	1,65%	2,2%
2,95%	0,93%	3,11%
6,38%	4,08%	3,8%

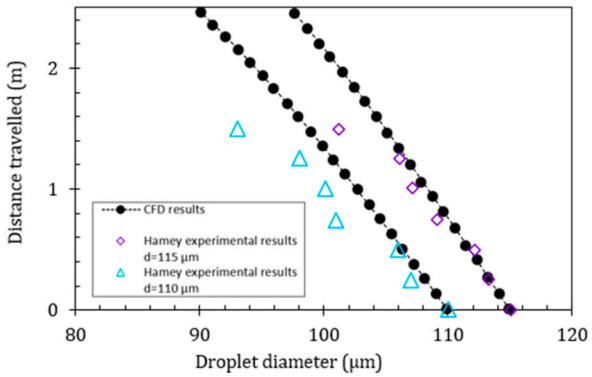

Fig. 9. Destination of drops of water. Experimental result of the study of Ref. [35] consisting of two droplets of pure water introduced into an environment of 70% relative humidity at a temperature of 20°C and dropped freely through a space to observe the distance they travel as they evaporate. The droplets have a diameter of 110 μm and 115 μm and have a temperature of 16°C.

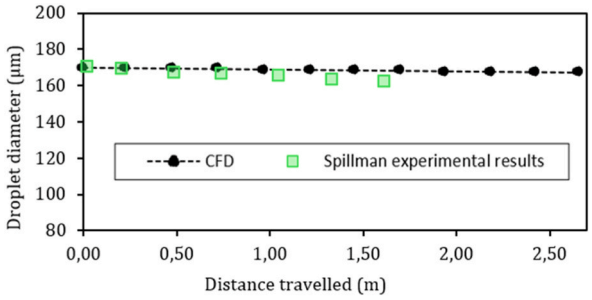

Fig. 10. Destination of water drops. Experimental study of Ref. [36] consisting of a droplet of pure water introduced into an environment of 68% relative humidity at a temperature of 31°C and is freely dropped down a space to observe the distance it travels as it evaporates. The drop has a diameter of 170 μm and a temperature of 25°C.

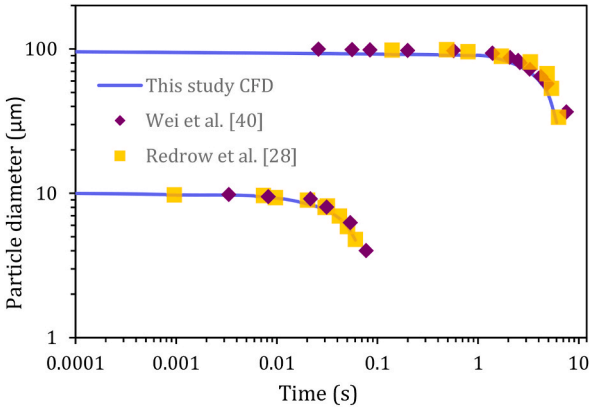

Fig. 11. Evaporation of pure water droplets. The ambient air temperature is 293.15 K, with a relative humidity of 0%. The droplets initial temperature is 310.15 K. The diameter of the droplets are 10 μm and 100 μm.

with mechanical ventilation. The saliva generated and expelled into the environment, either by speech or sneezing has the same characteristics and is modeled as a saline solution. The difference is that the aerosols generated by the student are contaminated. The results show in all three scenarios, that the largest particles fall to the ground while aerosols below 20 μm spread through the classroom environment. In contrast, particles larger than 500 μm travel through the classroom in the sneeze direction until they hit the wall, in less than 1 s. Fig. 12 shows the route of the aerosols in a classroom without ventilation, where the student placed a row later that the student infected is the most affected by them. In 0.5 s aerosols impregnate the student from the first row. Practically, for 4 s all aerosols fell to the floor. The particles generated in speech fall vertically without any external movement. When the ventilation used is natural,

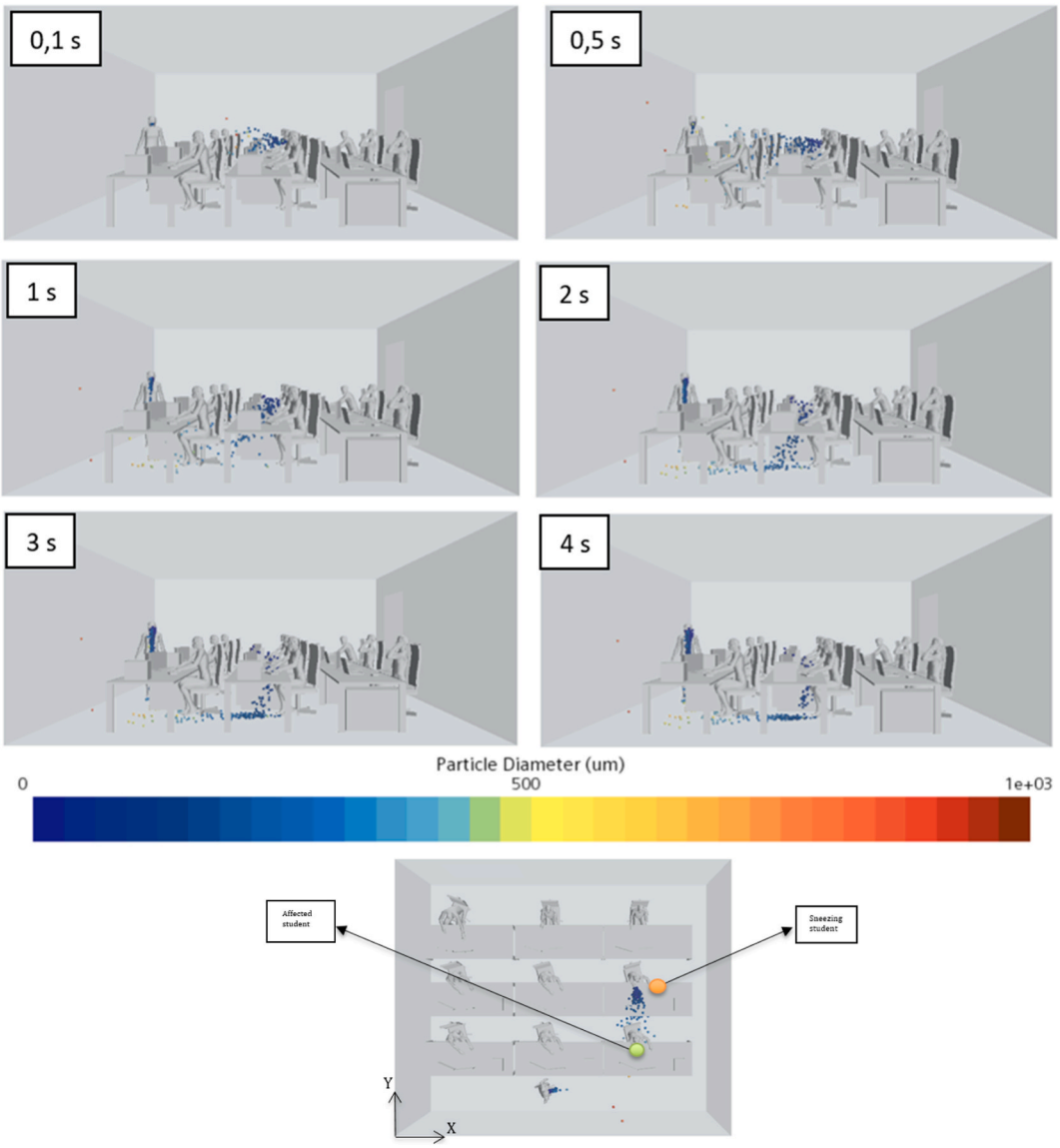

Fig. 12. Route and destination of aerosols generated in the classroom without ventilation. The student placed in the first row on the right is the most affected. Larger particles quickly fall to the ground.

the student placed in front of the student infected is the most affected. In this case, the particles collide with the wall 0.5 s, so it is seen that the student placed in the first row also receives them. After 2 s there is hardly any change in the scene, since for 1 s, all the particles have been deposited on the student's table in the first row, as can be seen in Fig. 13. The aerosols generated by speech take the opposite direction to the one thrown into the environment, until touching with the ceiling. Particles with a diameter greater than 500 μm are deposited under the first-row student's table, and as time passes their diameter decreases.

Finally, in Fig. 14, the aerosol path is provided when the room is subjected to mechanical ventilation. Aerosols take different routes. Contaminated particles with larger diameter fall on the table of the sneezing student. From 0.1 s to 0.5 s is the time interval where the first-row student is most exposed. From 3 s the aerosols of diameter less than 15 μm, by the pressure exerted by mechanical ventilation ascend towards the duct, sucking them. Aerosols expelled by the teacher's speech, as in the situation of no ventilation, fall vertically without any movement outside the normal. Fig. 15 shows those droplets that rise by the influence of the fan. The range of 3–4.5 s where the aerosol trajectory is noted is shown.

b. Mass of aerosols accumulated in different scenarios

The contaminated load that the infected person generated is a parameter of great importance to control to prevent infection in an easier way. CFDs have the limitation of not being able to give results in relation to this parameter. However, it is considered that a

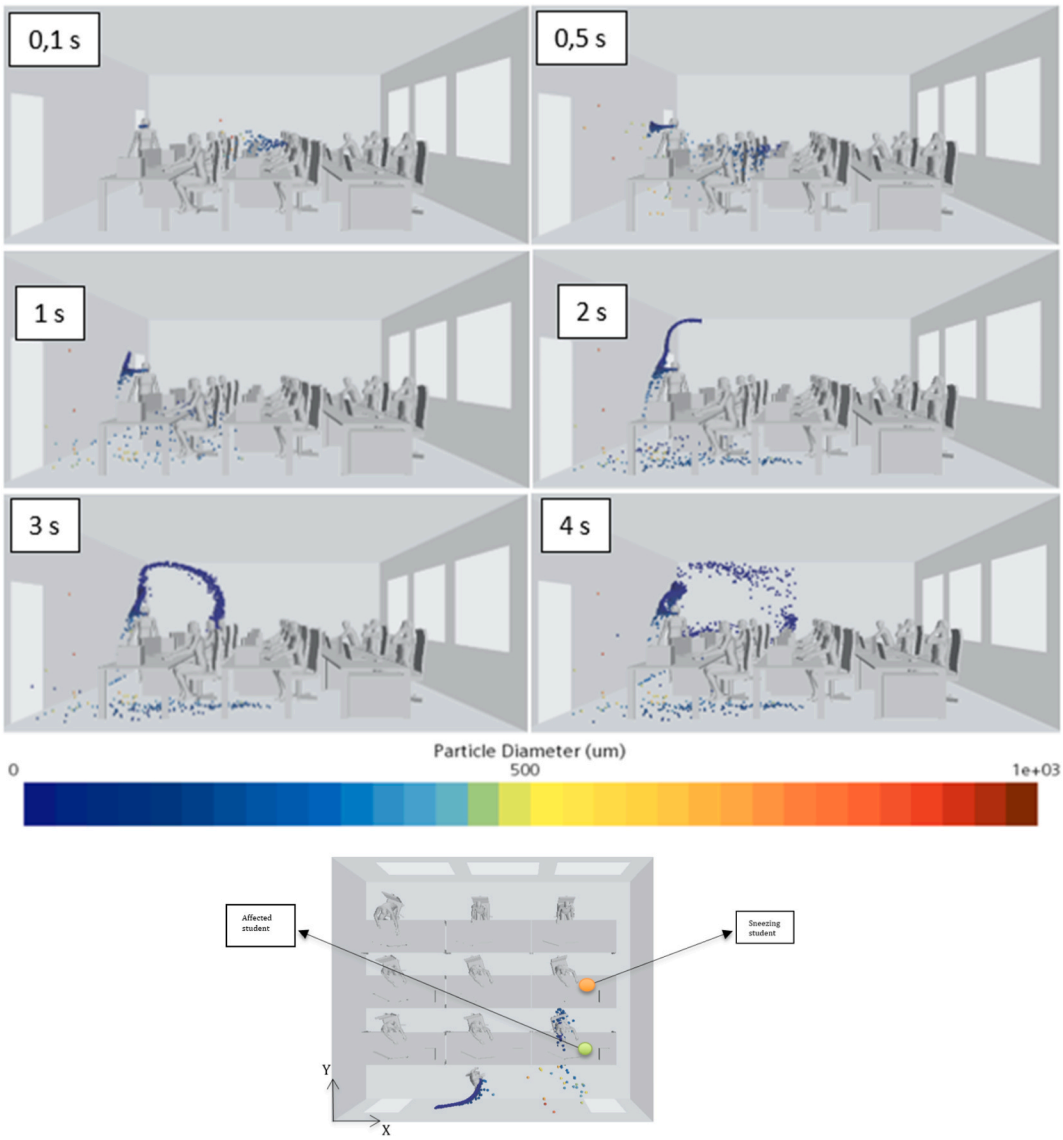

Fig. 13. Route and destination of aerosols generated in the classroom with natural ventilation. The student placed in the first row on the right is the most affected. The larger particles quickly fall to the ground. The aerosols generated by the teacher's speech take the opposite direction to the one poured.

given quantity of aerosols contains a specific mass in each time interval accumulated in the classroom in the three scenarios analyzed. Fig. 16, Figs. 17 and 18 indicate the mass of particles in the classroom without, with natural and with mechanical ventilation, respectively, for 3.5 s. Note that the vertical axis representing the particle count is defined in logarithmic scale. To analyze these data it has been chosen to analyze 0.5 s, since it is when the sneeze is completed and is the moment of time where the classroom contains more droplets. In 0.5 s, in the classroom without ventilation, shown in Fig. 16, there are about 9 million droplets with a mass of 0.0025 mg; the other masses are almost negligible because there are only 100 droplets having different mass. The largest mass obtained is 0.4 mg. The situation in the carrier with natural ventilation is approximately similar to the previous one, shown in Fig. 17. Where a clear difference is obtained in mechanical ventilation, there are 5.5 million particles dispersed in the air with a mass of 0.0028 mg, shown in Fig. 18. As in other cases, the other masses are made up of a negligible number of particles. In this scenario, the particles with the highest mass reach 0.45 mg. The amount of these particles is negligible, as shown in Fig. 19, the highest mass obtained in this scenario is 0.33 mg, present in 3.5 s. In all three cases it can be seen how, thanks to the phenomenon of evaporation, as time progresses the particles of lower mass increase.

c. Loss of energy

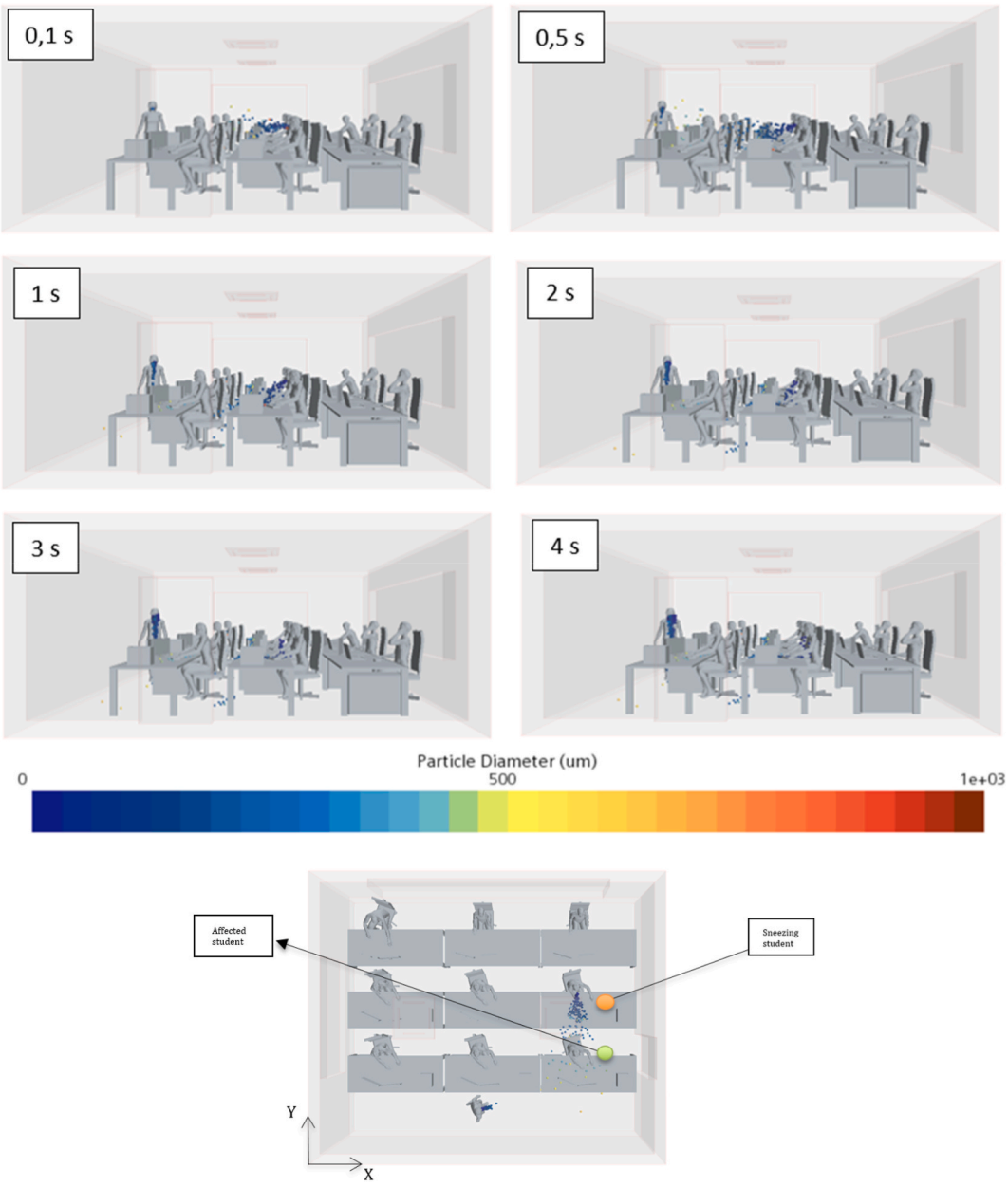

Fig. 14. Route and destination of aerosols generated in the classroom with mechanical ventilation. The student placed in the first row on the right is the most affected. Larger particles quickly fall on the infected student's table, due to the air inlet pressure generated by the ventilation duct.

It is not economically viable to take refuge in a classroom with excellent efficiency in the control of aerosols if the losses of energy exceed impossible numbers to cope with. Consequently, the energy loss generated in the carrier of the different three scenarios is calculated in the following subsection, to be able to define more accurately the scenario that best covers the two points described. Heat transfer through a flat wall can be considered as one-dimensional [45]. To calculate the energy losses generated in these cases, Fourier's law for conduction and Newton's law for cooling for convection have been used, shown in Equations (11) and (12), respectively.

$$\dot{Q}_{conduction} = \mathrm{A} \times \frac{T_{high} - T_{low}}{dX} \times \lambda \tag{11}$$

$$\dot{Q}_{convection} = \mathrm{A} \times \left(T_{high} - T_{low}\right) \times h \tag{12}$$

where λ is the thermal conductivity of the material, A is the area perpendicular to heat transfer (m^2), dX is the thickness of the material

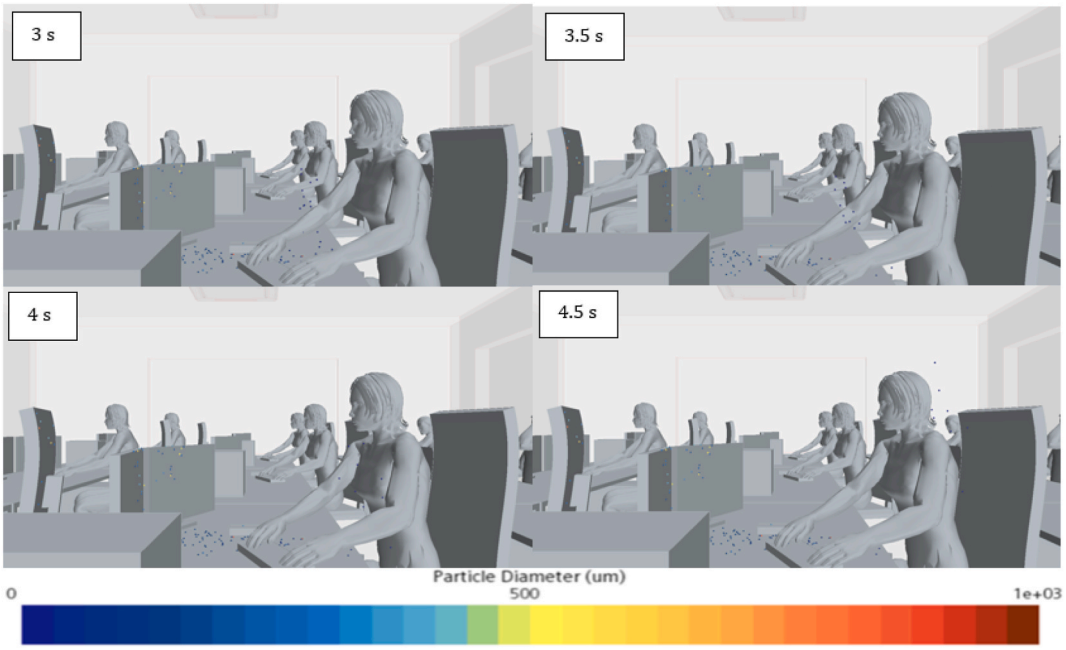

Fig. 15. Trajectory of aerosols in the class with a mechanical ventilation system. Detail of the movement of aerosols that are moved by the pressure exerted by the fan in the period of 3–4.5 s.

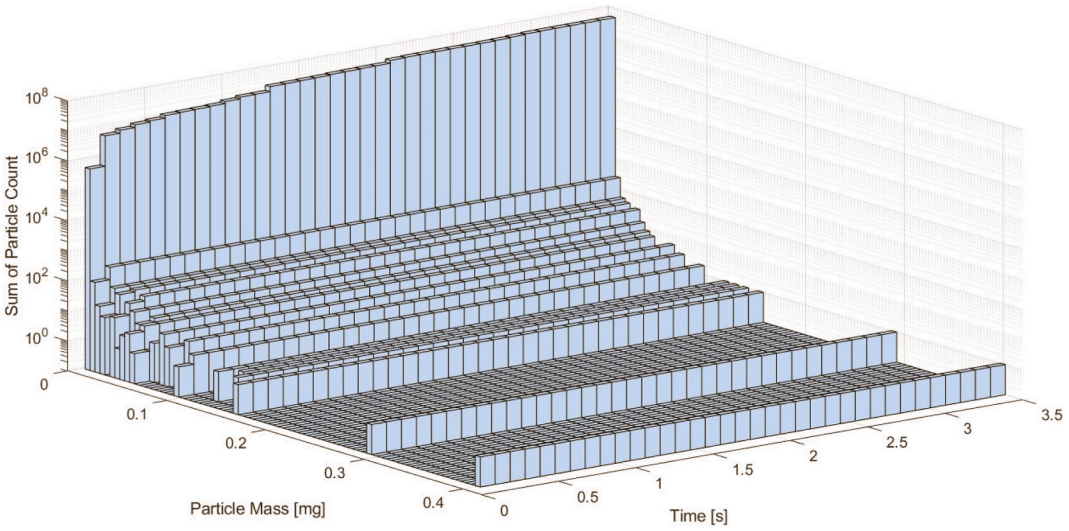

Fig. 16. Vertical axis in logarithmic scale. The amount of aerosols with a specific mass at each time interval in a non-ventilated classroom. Particles amount to a maximum mass of 0.4 mg.

(m) and h is the coefficient of heat transfer by convection. T_{high} refers to the indoor temperature and T_{low} at the outside temperature, in this case.

The data to take into account is the following; the total area of the windows that compose the classroom is 13,8 m^2 and consists of 2 crystals 8 mm thick, 2 cm apart. The thermal conductivity of the glass is 0.81 W/mK and the thermal conductivity of the air is 0.026 W/mK. The coefficient of heat transfer by convection between crystals takes the value of 4 W/m^2K and outside 15 W/m^2K. The temperature inside the room is 21 °C and the outside temperature is 17 °C, whereas when there is mechanical ventilation, the inside temperature drops to 19 °C. Considering this, the results obtained are shown below, consequence of the sum of the two equations, being a problem with conduction and convection.

$$-\dot{Q_l} = 38.8\ W$$

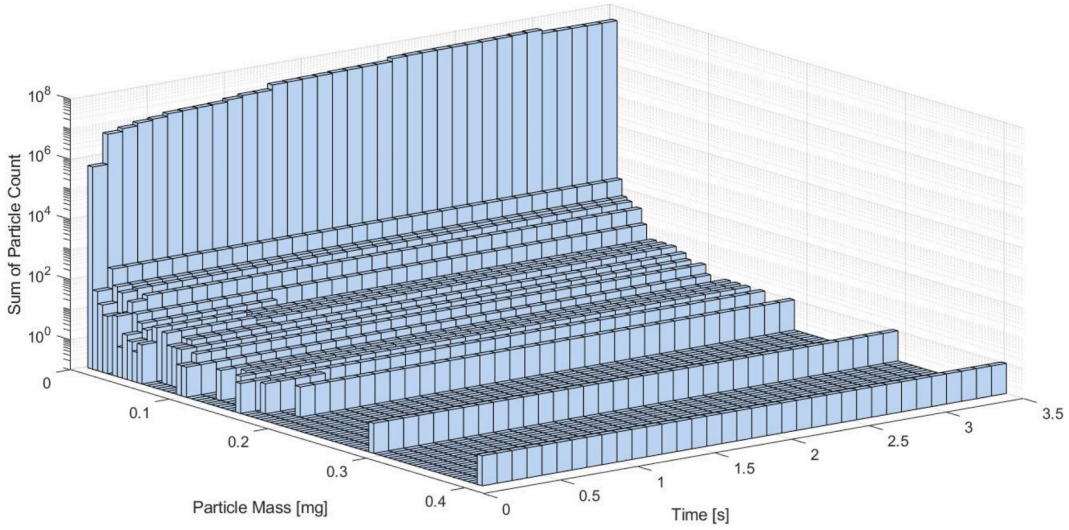

Fig. 17. Vertical axis in logarithmic scale. The amount of aerosols with a specific mass at each time interval in a naturally ventilated classroom. Particles amount to a maximum mass of 0.4 mg.

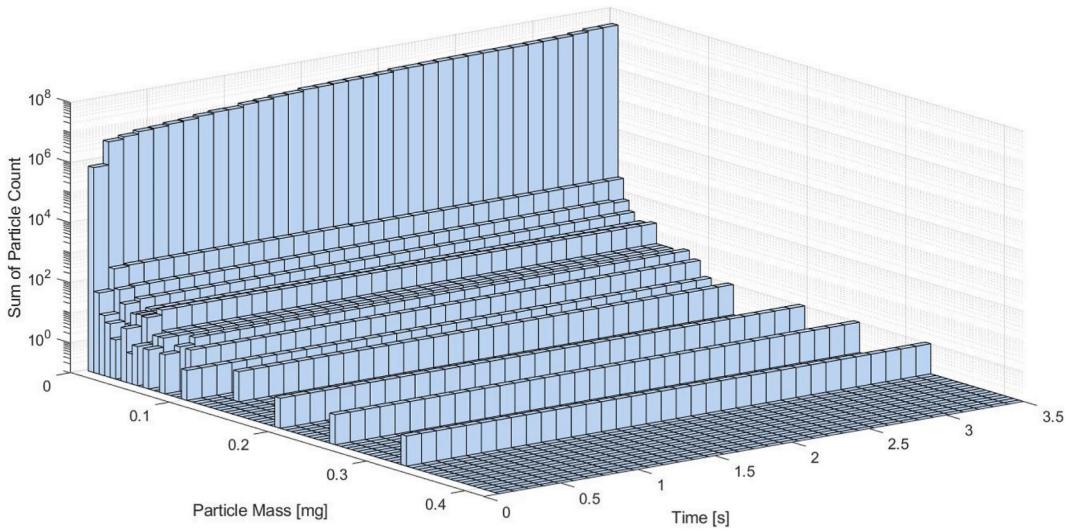

Fig. 18. Vertical axis in logarithmic scale. The amount of aerosols with a specific mass at each time interval in a mechanically ventilated classroom. Particles amount to a maximum mass of 0.33 mg.

$$-\dot{Q_2} = 19.4 \text{ W}$$

$$-\dot{Q_3} = 828 \text{ W}$$

where $\dot{Q_1}$ is the loos of energy of the classroom without ventilation, $\dot{Q_2}$ is the loos of energy of the classroom with mechanical ventilation and $\dot{Q_3}$ corresponds to the energy of the classroom with natural ventilation.

According to the previous results, a temperature variation between outside and inside the room is responsible for generating energy losses. The heat generated in a closed room, independent of the temperature, is more efficient than a room with open spaces to the outside. Therefore, the results are staggered depending on the temperature difference.

4. Conclusion

A numerical model based on Eulerian-Lagrangian techniques is presented in the current study. The efficiency of the different ventilation strategies for an efficient control of aerosols dispersion is analyzed. The domain, composed of nine students and one

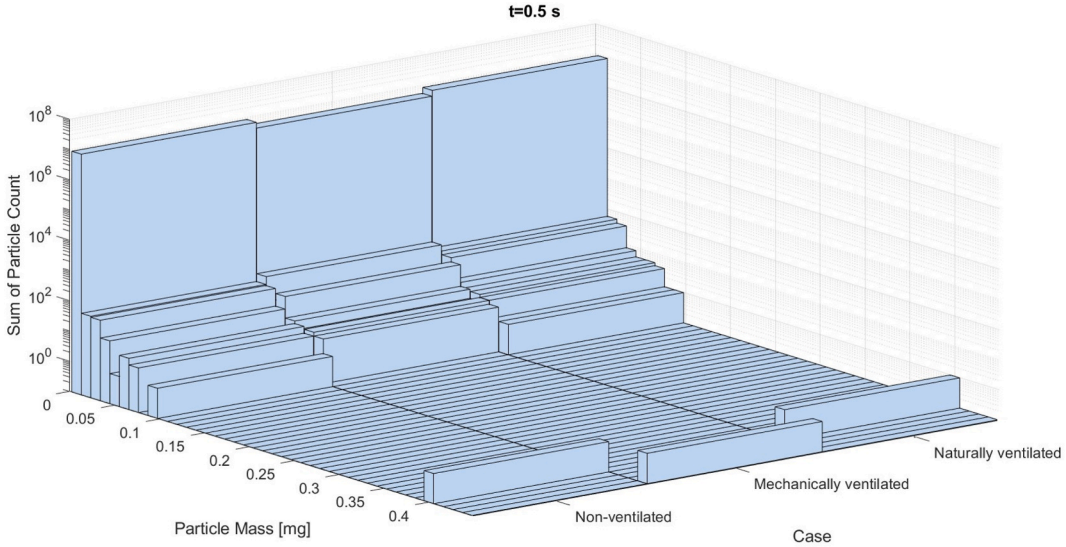

Fig. 19. Mass of droplets accumulated in all three scenarios at the instant 0.5 s. The scenario with mechanical ventilation totals 5.5 million particles with a mass of approximately 0.0028 mg. On the other hand, in the scenario with natural ventilation and without ventilation 9 million particles with a mass of 0.0025 mg are measured.

teacher, is at a temperature of 21 °C and a relative humidity of 42%. The main result observed is that a classroom with a mechanical ventilation scheme is the best place to protect healthy people from a contaminated sneeze. With the student distribution assigned to this set up, the particles exhaled to the environment take different routes, most are thrown on the table of the student infected, thus preventing the tour of the classroom. This is due to outside air being injected into the classroom from the ceiling. With natural ventilation, the particles tend to catch more speed due to the external air coming through the windows, thus helping a greater exposure of particles in the environment. It should be noted that, the scenario with natural ventilation is the most unfavorable of the three cases analyzed, taking into account that has been simulated with a specific air speed, direction, pressure and temperature. As a result of a lower temperature, although, the relative humidity remains constant, in the classroom due to the injection of mechanical ventilation air, the mass that accumulates in the carrier is greater when the ventilation is mechanical. The evaporation process of the droplets injected into the environment is performed at a shorter time. The data show that both, in the scenario without ventilation and with natural ventilation, the accumulated mass is similar in the 4 s simulated in this project, so the big difference that is obtained in these two scenarios is the route and destination of the aerosols.

Consequently, in order to analyzing energy losses in the classroom, the scenario with mechanical ventilation is the least. It happened because the temperature difference between the classroom and the outside is smaller. In the case of natural ventilation, the energy losses generated are high compared to the other two cases. Therefore, it can be concluded that mechanical ventilation is a good measure to carrying a control of aerosols in the presented classroom. With nine students in three rows of three students, separated by 1.5 m between them, the classroom without ventilation or with a natural ventilation, exposed specific conditions of relative humidity, temperature and air direction provides less efficient results.

Funding

The authors are thankful to the government of the Basque Country for the financial support of ELKARTEK21/10 KK-2021/00014 and ELKARTEK20/78 KK-2020/00114 research programs, respectively.

Author contribution statement

Ainara Ugarte-Anero; Unai Fernandez Gamiz: Conceived and designed the experiments; Performed the experiments; Analyzed and interpreted the data; Contributed reagents, materials, analysis tools or data; Wrote the paper. Koldo Portal-Porras: Conceived and designed the experiments; Contributed reagents, materials, analysis tools or data. Jose Manuel Lopez-Guede: Performed the experiments; Wrote the paper. Gaspar Sanchez-Merino: Analyzed and interpreted the data.

Data availability statement

Data will be made available on request.

Declaration of competing interest

The authors declare that they have no known competing financial interests or personal relationships that could have appeared to influence the work reported in this paper.

Acknowledgements

The authors are grateful for the support provided by the SGIker of UPV/EHU.

Appendix A. Nomenclature

Symbol	*Definition (units)*
φ_i	value of the property of the mixture
Y_i	the mass fraction of dry air and water vapor
σk	terms of production
σω	terms of production
Pk	terms of production
P_ω	terms of production
Sk	source term
Sω	source term
k0	environmental turbulence value
ω0	environmental turbulence value
$\overline{v}$	average speed (m/s)
μ	dynamic viscosity (kg/ms)
$f_{\beta*}$	free shear modification factor
v	continuous speed
f_b	result of the forces of the body per unit of volume acting on the continuous (N/m3)
σ	tension (N/m2)
p	pressure (Pa)
T	viscous tensor (kg/ms)
E	energy per unit of mass (J/kg)
q	heat flow (J/s)
S_E	one energy source per unit volume (J/m3)
F_d	drag (N)
C_d	drag coefficient
ρ	density (kg/m3)
A_p	area of the droplet (m2)
v_s	sliding speed of the drop (m/s)
$\dot{m}_p$	mass of droplets (g/s)
B	Spalding transfer number
g^*	mass transfer conductance (g/m2 s)
A_s	surface of the drop (m2)
$P_{va,s}$	saturation pressure of the drop in the salt mixture (Pa)
P_{va}	equilibrium pressure of the water (Pa)
X_d	molar fraction of the drop
Mw	molecular weight of water (u)
Ms	molecular weight of solute (u)
ms	mass of solute in the drop (g)
d_p	diameter of the drop (m)
i	ionic factor
ƛ	thermal conductivity of the material (WmK)
A	area perpendicular to heat transfer (m2)
dX	the thickness of the material (m)
h	the coefficient of heat transfer by convection W/m2K
$\dot{Q}_x$	energy loss (W)
RH	Relative humidity (%)
CFD	Computational Fluid Dynamics
WHO	World Health Organization
ACH	Air Change per Hour

References

[1] M.Z. Abouleish, Indoor air quality and COVID-19, Publ. Health 191 (2021) 1.
[2] J. Liu, Z. Lin, Energy and exergy analyze of different air distributions in a residential building, Energy Build. 233 (2021), 110694.
[3] P. Wargocki, J. Sundell, W. Bischof, G. Brundrett, P.O. Fanger, F. Gyntelberg, S.O. Hanssen, P. Harrison, A. Pickering, O. Seppänen, Ventilation and health in non-industrial indoor environments: report from a European multidisciplinary scientific consensus meeting (EUROVEN), Indoor Air 12 (2002) 113–128.
[4] R.K. Bhagat, M.S. Davies Wykes, S.B. Dalziel, P.F. Linden, Effects of ventilation on the indoor spread of COVID-19, J. Fluid Mech. 903 (2020) F1, https://doi.org/10.1017/jfm.2020.720. Available online: https://www.cambridge.org/core/article/effects-of-ventilation-on-the-indoor-spread-of-covid19/CF272DAD7C27DC44F6A9393B0519CAE3, 2022/07/06.
[5] N. Agarwal, C.S. Meena, B.P. Raj, L. Saini, A. Kumar, N. Gopalakrishnan, A. Kumar, N.B. Balam, T. Alam, N.R. Kapoor, V. Aggarwal, Indoor air quality improvement in COVID-19 pandemic: review, Sustain. Cities Soc. 70 (2021), 102942, https://doi.org/10.1016/j.scs.2021.102942. https://www.sciencedirect.com/science/article/pii/S2210670721002274. Available online.
[6] A. Ugarte-Anero, U. Fernandez-Gamiz, K. Portal-Porras, E. Zulueta, O. Urbina-Garcia, Computational characterization of the behavior of a saliva droplet in a social environment, Sci. Rep. 12 (2022) 1–14.
[7] H. Motamedi, M. Shirzadi, Y. Tominaga, P.A. Mirzaei, CFD modeling of airborne pathogen transmission of COVID-19 in confined spaces under different ventilation strategies, Sustain. Cities Soc. 76 (2022), 103397, https://doi.org/10.1016/j.scs.2021.103397. https://www.sciencedirect.com/science/article/pii/S2210670721006703. Available online.
[8] G.M. Abbas, I.G. Dino, The impact of natural ventilation on airborne biocontaminants: a study on COVID-19 dispersion in an open office, Eng. Construct. Architect. Manag. 29 (2021) 1609–1641.
[9] G.M. Abbas, I. Gursel Dino, COVID-19 dispersion in naturally-ventilated classrooms: a study on inlet-outlet characteristics, Journal of Building Performance Simulation 15 (2022) 656–677.
[10] K. Li, W. Xu, L. Song, X. Zhang, C. Zhang, J. Hua, Numerical study of spread of coughing droplets by human walking and indoor wind environment, Phys. Fluids (2023) 35.
[11] Q. Zhou, H. Qian, L. Liu, Numerical investigation of airborne infection in naturally ventilated hospital wards with central-corridor type, Indoor Built Environ. 27 (2018) 59–69.
[12] M. Mirzaie, E. Lakzian, A. Khan, M.E. Warkiani, O. Mahian, G. Ahmadi, COVID-19 spread in a classroom equipped with partition – a CFD approach, J. Hazard Mater. 420 (2021), 126587, https://doi.org/10.1016/j.jhazmat.2021.126587. https://www.sciencedirect.com/science/article/pii/S0304389421015521. Available online.
[13] C.K. Ho, Modelling airborne transmission and ventilation impacts of a COVID-19 outbreak in a restaurant in Guangzhou, China, Int. J. Comput. Fluid Dynam. 35 (2021) 708–726.
[14] A. Pal, R. Biswas, R. Pal, S. Sarkar, A. Mukhopadhyay, A novel approach to preventing SARS-CoV-2 transmission in classrooms: a numerical study, Phys. Fluids 35 (2023), 013308.
[15] S. Srivastava, X. Zhao, A. Manay, Q. Chen, Effective ventilation and air disinfection system for reducing coronavirus disease 2019 (COVID-19) infection risk in office buildings, Sustain. Cities Soc. 75 (2021), 103408, https://doi.org/10.1016/j.scs.2021.103408. https://www.sciencedirect.com/science/article/pii/S2210670721006818. Available online.
[16] M. Romero-Flores, E.A. López-Guajardo, A. Delgado-Gutiérrez, A. Montesinos-Castellanos, Strategies for reducing airborne disease transmission during breathing using a portable air cleaner in a classroom, Phys. Fluids 35 (2023), 15137, https://doi.org/10.1063/5.0134611. Available online:.
[17] Precio de la luz: las facturas siguen al alza.Available online: https://www.ocu.org/vivienda-y-energia/gas-luz/informe/precio-luz..
[18] El 99% de las viviendas españolas sufre pérdidas de calor innecesarias.Available online: https://www.elmundo.es/economia/2016/01/20/569f66c8ca47412d618b45dc.html..
[19] S.A. Chillón, A. Ugarte-Anero, I. Aramendia, U. Fernandez-Gamiz, E. Zulueta, Numerical modeling of the spread of cough saliva droplets in a calm confined space, Mathematics 9 (2021) 574, https://doi.org/10.3390/math9050574. Available online: https://search.proquest.com/docview/2501480547.
[20] T. Dbouk, D. Drikakis, On coughing and airborne droplet transmission to humans, 53310-53310, Phys. Fluids (32) (2020), https://doi.org/10.1063/5.0011960. Available online:.
[21] G. Busco, R. Yang, J. Seo, Y.A. Hassan, Sneezing and asymptomatic virus transmission, Phys. Fluids (2020) 32.
[22] Z.Y. Han, W.G. Weng, Q.Y. Huang, Characterizations of particle size distribution of the droplets exhaled by sneeze, J. R. Soc. Interface 10 (2013), 20130560.
[23] J.K. Gupta, C. Lin, Q. Chen, Characterizing exhaled airflow from breathing and talking, Indoor Air 20 (2010) 31–39.
[24] C.Y.H. Chao, M.P. Wan, L. Morawska, G.R. Johnson, Z.D. Ristovski, M. Hargreaves, K. Mengersen, S. Corbett, Y. Li, X. Xie, Characterization of expiration air jets and droplet size distributions immediately at the mouth opening, J. Aerosol Sci. 40 (2009) 122–133.
[25] M.R.O. Panão, Why drop size distributions in sprays fit the lognormal, Phys. Fluids 35 (2023), 11701, https://doi.org/10.1063/5.0135510. Available online:.
[26] S. Zhu, S. Kato, J. Yang, Study on transport characteristics of saliva droplets produced by coughing in a calm indoor environment, Build. Environ. 41 (2006) 1691–1702, https://doi.org/10.1016/j.buildenv.2005.06.024. Available online:.
[27] A. Ugarte-Anero, U. Fernandez-Gamiz, I. Aramendia, E. Zulueta, J.M. Lopez-Guede, Numerical modeling of face shield protection against a sneeze, Mathematics 9 (2021) 1582.
[28] J. Redrow, S. Mao, I. Celik, J.A. Posada, Z. Feng, Modeling the evaporation and dispersion of airborne sputum droplets expelled from a human cough, Build. Environ. 46 (2011) 2042–2051.
[29] X. Xie, Y. Li, A. T. Y. Chwang, P. L. Ho, E. H. Seto How far droplets can move in indoor environments-revisiting the Wells evaporation-falling curve. , DOI 10.1111/j.1600-0668.2006.00469.x..
[30] H. Li, F.Y. Leong, G. Xu, Z. Ge, C.W. Kang, K.H. Lim, Dispersion of evaporating cough droplets in tropical outdoor environment, Phys. Fluids (32) (2020), 113301, https://doi.org/10.1063/5.0026360. Available online:.
[31] A. Foster, M. Kinzel, Estimating COVID-19 exposure in a classroom setting: a comparison between mathematical and numerical models, Phys. Fluids 33 (2021), 021904.
[32] J. Kukkonen, T. Vesala, M. Kulmala, The interdependence of evaporation and settling for airborne freely falling droplets, J. Aerosol Sci. 20 (1989) 749–763, https://doi.org/10.1016/0021-8502(89)90087-6. https://www.sciencedirect.com/science/article/pii/0021850289900876. Available online.
[33] F.R. Menter, Two-equation eddy-viscosity turbulence models for engineering applications, AIAA J. 32 (1994) 1598–1605, https://doi.org/10.2514/3.12149. Available online: http://arc.aiaa.org/doi/full/10.2514/3.12149.
[34] B. Wang, H. Wu, X. Wan, Transport and fate of human expiratory droplets-A modeling approach, Phys. Fluids (2020) 32.
[35] P.Y. Hamey, The Evaporation of Airborne Droplets, Granfield Institute of Technology, Bedfordshire, 1982.
[36] Spillman Evaporation from freely falling droplets, Aeronaut. J. 88 (1984) 181–185.
[37] S. Kumar, M.D. King, Numerical investigation on indoor environment decontamination after sneezing, Environ. Res. 213 (2022), 113665.
[38] R. Bale, A. Iida, M. Yamakawa, C. Li, M. Tsubokura, Quantifying the COVID19 infection risk due to droplet/aerosol inhalation, Sci. Rep. 12 (2022), 11186.
[39] Y. Yang, N. Zhu, Y. Wang, Y. Wei, Inhalation and deposition of gas–droplet contaminant in the human microenvironment in an industrial building, Indoor Built Environ 32 (7) (2023) 1393–1410, https://doi.org/10.1177/1420326X231160266.
[40] J. Wei, Y. Li, Enhanced spread of expiratory droplets by turbulence in a cough jet, Build. Environ. 93 (2015) 86–96, https://doi.org/10.1016/j.buildenv.2015.06.018. Available online:.
[41] N. Sen, Transmission and evaporation of cough droplets in an elevator: numerical simulations of some possible scenarios, Phys. Fluids 33 (2021), 033311, https://doi.org/10.1063/5.0039559. Available online:.
[42] Y. Yan, X. Li, J. Tu, Thermal effect of human body on cough droplets evaporation and dispersion in an enclosed space, Build. Environ. 148 (2019) 96–106.

[43] X. Li, Y. Shang, Y. Yan, L. Yang, J. Tu, Modelling of evaporation of cough droplets in inhomogeneous humidity fields using the multi-component Eulerian-Lagrangian approach, Build. Environ. 128 (2018) 68–76.
[44] Z. Liu, J. Wu, G. Yang, X. Zhang, Z. Dai, A numerical study of COVID-19-laden droplets dispersion in aircraft cabin ventilation system, Heliyon 9 (2023).
[45] Y.A. Cengel, A.J. Ghajar, Transferencia de calor y masa, McGraw-Hill Interamericana, 2007.